Excited intruder states in ^{32}Mg

Vandana Tripathi, S. L. Tabor, P. Bender, C. R. Hoffman, Sangjin Lee, K. Pepper, and M. Perry
Department of Physics, Florida State University, Tallahassee, Florida 32306, USA

P. F. Mantica,[1,2] J. M. Cook,[1,3] J. Pereira,[1] J. S. Pinter,[1,2] J. B. Stoker,[1,2] and D. Weisshaar[1]
[1]*National Superconducting Cyclotron Laboratory, Michigan State University, East Lansing, Michigan 48824, USA*
[2]*Department of Chemistry, Michigan State University, East Lansing, Michigan 48824, USA*
[3]*Department of Physics, Michigan State University, East Lansing, Michigan 48824, USA*

Y. Utsuno
Advanced Science Research Centre, Japan Atomic Energy Agency, Tokai, Ibaraki 319-1195, Japan

T. Otsuka
Department of Physics and Center for Nuclear Study, University of Tokyo, Hongo, Tokyo 113-0033, Japan and RIKEN, Hirosawa, Wako-shi, Saitama 351-0198, Japan

(Received 13 December 2007; published 24 March 2008)

The low energy level structure of $N = 20$ ^{32}Mg obtained via β-delayed γ spectroscopy is reported. The level structure of ^{32}Mg is found to be completely dominated by intruders. An inversion between the 1p-1h and 3p-3h states is observed for the negative parity states, similar to the 0p-0h and 2p-2h inversion for the positive parity states in these $N \sim 20$ nuclei. The intruder excited states, both positive and negative parity, are reasonably explained by Monte Carlo shell model calculations, which suggest a shrinking $N = 20$ shell gap with decreasing Z.

DOI: 10.1103/PhysRevC.77.034310 PACS number(s): 23.40.−s, 21.60.Cs, 23.20.Lv, 27.30.+t

I. INTRODUCTION

In the β decay of ^{30}Na and ^{32}Na studied by Detraz *et al.* [1], the most prominent γ rays were assigned to the $2^+ \rightarrow 0^+$ transition in the daughter nuclei, ^{30}Mg and ^{32}Mg, respectively. The 2^+ state in ^{32}Mg measured at 885 keV came as a surprise, as it showed a sudden dip from ^{30}Mg (see Fig. 1), not expected for this singly magic nuclei with $N = 20$. It was also inconsistent with shell model calculations within the *sd* space [2] that predict the first 2_1^+ state in ^{32}Mg at 1.67 MeV. The 885 keV 2_1^+ state in ^{32}Mg is also in sharp contrast with nearby $N = 20$ isotones like ^{34}Si (3.328 MeV) or ^{36}S (3.291 MeV) or ^{38}Ar (2.167 MeV). The low 2_1^+ state in ^{32}Mg can be taken as evidence of unexpected increased deformation of this isotope. With two extra protons, ^{34}Si displays the expected trend at $N = 20$ (Fig. 1). Later in an intermediate energy Coulomb excitation experiment at RIKEN [3], the $B(E2; 0_1^+ \rightarrow 2_1^+) = 454\,(78)\ e^2\ \mathrm{fm}^4$ was measured for ^{32}Mg, corresponding to $\beta_2 \approx 0.5$ in the rigid rotor model, suggesting a large prolate deformation.

^{32}Mg is not isolated in its anomalous properties. The large deformation of other $N \sim 20$ isotopes like ^{31,32,34}Mg [4–6] and ^{30}Ne [7] along with the irregular ground state properties of ^{31,32}Na [8,9] indicates a region of $N \sim 20$ isotopes of Ne, Na, and Mg with such properties, referred to as the *island of inversion* [10]. Even for the neutron-rich fluorine isotopes, a tendency toward deformation has been suggested by the stability of ^{31}F with $N = 22$, in contrast to the particle unstable nature of ^{25}O with $N = 17$ [11].

The properties of these neutron-rich *sd*-shell nuclei can be explained if mixing of an excited "intruder" configuration involving neutrons in the *fp* shell is included. This indicates a narrow $N = 20$ shell gap, highlighting the change in shell structure moving away from the β-stable nuclei toward the drip line. Both mean field and shell models have been put to the test to explain the properties of these nuclei with large isospin. The mean field calculation with monopole interaction reproduced the disappearance of the $N = 20$ shell closure in the Mg isotopes [12]. In shell model studies [13–16], the effect of 2p-2h excitations enhanced by the narrow shell gap across $N = 20$ has been postulated to promote the occurrence of the island of inversion. In the Monte Carlo shell model (MCSM) calculations [14–16], the spin-isospin property of the effective nucleon-nucleon interaction, which has its origin in the tensor interaction [17], has been the driving force behind this changing shell structure as a function of proton number for $N \sim 20$.

Considered inside the island of inversion, the level structure of ^{32}Mg has been the focus of many studies over the years. The information about excited states in ^{32}Mg from the literature is displayed in Fig. 2 and, as can be seen, there is no consensus between the various data sets beyond the first excited state, 2^+ at 885 keV. The β-decay investigation of Klotz *et al.* [18], based on the allowed nature of the log *ft* values, suggested that all the levels above 885 keV have negative parity because the parent nucleus ^{32}Na has negative parity. A recent β-decay study [19], published during the analysis of the present work, marked some differences with the earlier level structure in the energies of the excited states, though no log *ft* values or spin-parity assignments were presented. Studies that produced ^{32}Mg at high velocity in fragmentation reactions seem to

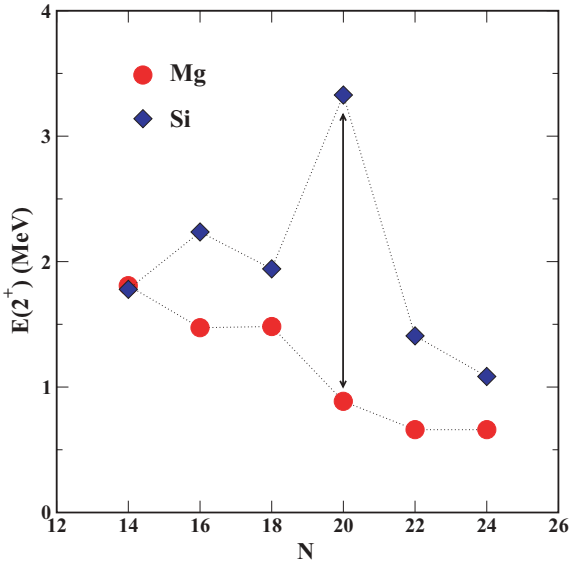

FIG. 1. (Color online) Systematics of the 2_1^+ energies in even-even neutron-rich Mg and Si isotopes (for $N = 14$–24). The data are from http://www.nndc.bnl.gov/ensdf/.

suggest positive parity for some states above 885 keV in contradiction to Ref. [18]. The in-flight spectroscopy [21] and the two-proton knockout from ^{34}Si [22] suggested a 4^+ state at 2.3 MeV, which they identify in energy with the 2321 keV state observed in the β decay. The Coulomb excitation experiment [4] proposed $1^\pm, 2^+$ for the 2321 keV excited state, as direct population of the 4^+ is expected to have a small cross section, whereas the strong population in nuclear inelastic scattering suggested a collective 3^- (1p-1h) state [23]. However, a recent analysis of proton inelastic scattering [24] implies a $\Delta L = 4$ transition rather than a $\Delta L = 3$ transition from the ground state to the 2321 keV state, making it a 4^+ state. Thus the divergence between the experimental results is far too great to come to any conclusion about the level structure or the collective nature of ^{32}Mg.

In this article, we report the study of excited states in ^{32}Mg via β^--delayed γ spectroscopy, which helps in resolving the above-mentioned discrepancies. A revision of spin and parity assignments brings most of the experimental data into agreement. The MCSM calculations with the SDPF-M interaction [14] provide a good explanation for the observed positions of the positive and negative parity states, indicating that most of the states have a dominant intruder character. However, the distribution of the Gamow Teller (GT) strength is not adequately reproduced. Comparison of the experimental data with the calculations suggests that the yrast negative parity states seen around ~3 MeV have a predominant 3p-3h configuration, implying an inversion in the negative parity states similar to the 2p-2h and 0p-0h inversions seen for the positive parity states.

II. EXPERIMENT

The β decay of ^{32}Na was studied at the National Superconducting Cyclotron Laboratory (NSCL) at Michigan State University. A 140 MeV/nucleon fully stripped ^{48}Ca primary beam from the coupled cyclotrons was fragmented in a

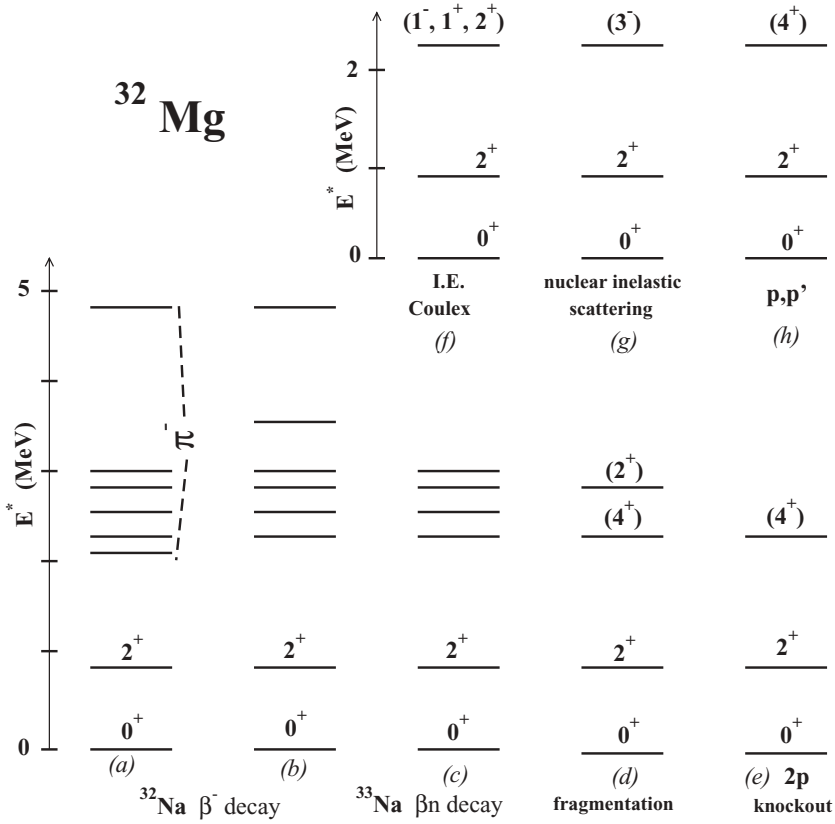

FIG. 2. Excited states of ^{32}Mg observed in various experiments: (a,b) β decay of ^{32}Na [18,19], (c) β-delayed neutron emission from ^{33}Na [20], (d) in-flight spectroscopy following fragmentation at GANIL [21], (e) two-proton knockout from ^{34}Si at MSU [22], (f) intermediate energy Coulomb excitation at MSU [4], (g) nuclear inelastic scattering [23], and (h) proton inelastic scattering in inverse kinematics at RIKEN [24].

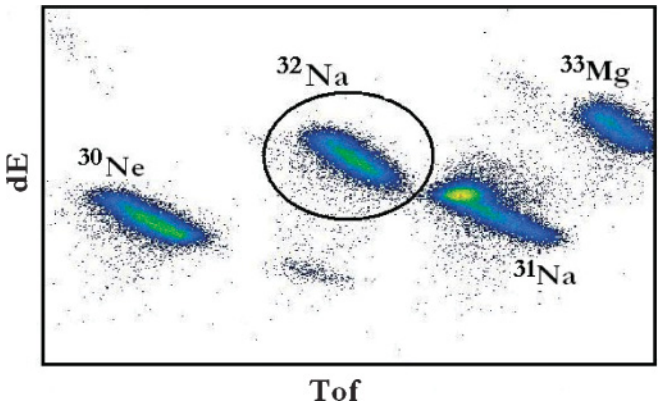

FIG. 3. (Color online) Two-dimensional particle identification plot of energy loss (ΔE) vs time-of-flight (Tof) for implantations that have a correlated β decay. The ^{32,31}Na groups were the strongest with the 2% momentum acceptance setting of the A1900. The other nuclides of the cocktail secondary beam were ^{30}Ne and ^{33}Mg.

752 mg/cm^2 Be target at the object of the A1900 [25]. The magnetic fields of the A1900 ($B\rho = 4.7856$ Tm and 4.6558 Tm), along with the 300 mg/cm^2 Al wedge at the intermediate image of the A1900, filtered the fragmentation products to produce a cocktail beam of the exotic nuclides ^{32,31}Na, ^{30}Ne, and ^{33}Mg. The secondary fragments were then transported to the experimental area where they were implanted in a 985- μm-thick 40 $\times$ 40 double-sided silicon strip detector (DSSD), the heart of the Beta Counting System (BCS) [26]. A particle identification spectrum obtained just before implantation is shown in Fig. 3, where ΔE was recorded in a PIN detector placed upstream of the DSSD. The time-of-flight (TOF) was recorded between this PIN detector and the rf signal from the cyclotron. The fragments that had around 100 MeV/nucleon energy had to be slowed down by passing through a thick Al degrader just before the DSSD to ensure implantation within the DSSD. The implants then decayed in the DSSD where the ensuing β particles were also detected. The preamplifiers reading the DSSD strips have two gain settings, one low and the other high to distinguish between the high-energy fragments and the low-energy β particles. Each event was tagged with an absolute time stamp generated by a free-running clock (50 MHz), which was the input of a 32-bit scaler channel. This allowed for correlations to be generated between the implants and decay events later in the software. The time differences between the arrival of each fragment and its subsequent decay were histogrammed to generate a decay curve.

The decay curve for the ^{32}Na implantations is shown in Fig. 4 for a period of 1 s. Being far from the β-stability line, the daughter nuclei are also radioactive with short half-lives and, hence, the initial decay of ^{32}Na is followed by a series of daughter and grand daughter decays. Also the very large Q_β value of 20.019 (357) MeV [27] is expected to lead to a large β-delayed neutron emission [18]. Taking into account the daughter and grand daughter decays and also the decay of the daughter nuclei produced after one- and two-neutron emissions, the decay curve was fitted to extract the half-life of ^{32}Na. The value obtained, 13.1 (5) ms, is in good agreement with the previously reported value of 13.2 (4) ms [28] and

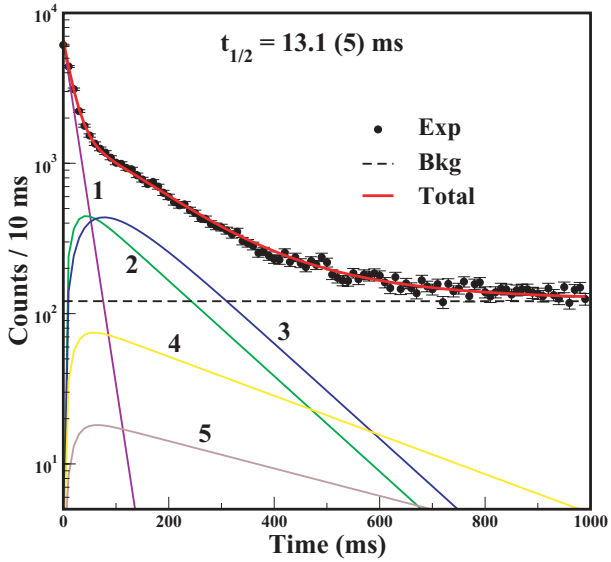

FIG. 4. (Color online) Decay curve of the ^{32}Na implants. The components of the fit that lead to a half-life determination of 13.1 (5) ms are: 1, ^{32}Na decay; 2, ^{32}Mg decay [95 (16) ms]; 3, ^{32}Al decay [33 (4) ms]; 4, ^{31}Mg decay [230 (20) ms]; and 5, ^{30}Mg decay [335 (17) ms]. ^{31}Mg and ^{30}Mg result from β-delayed 1n and 2n emissions, respectively.

consistent with that obtained with an additional constraint of observing the $2^+ \rightarrow 0^+$ transition in ^{32}Mg (Fig. 5). The number of β-decaying implants was also obtained from the fit to the total decay curve.

The γ rays following the β decay of the ^{30}Ne implants were recorded in 16 detectors of the SEgmented Germanium Array (SEGA) [29] packed closely around the BCS. In this geometry the efficiency of the array was about 20% at 200 keV and 7% at 1 MeV, which was calibrated with the help of standard sources. As noted before, due to the large

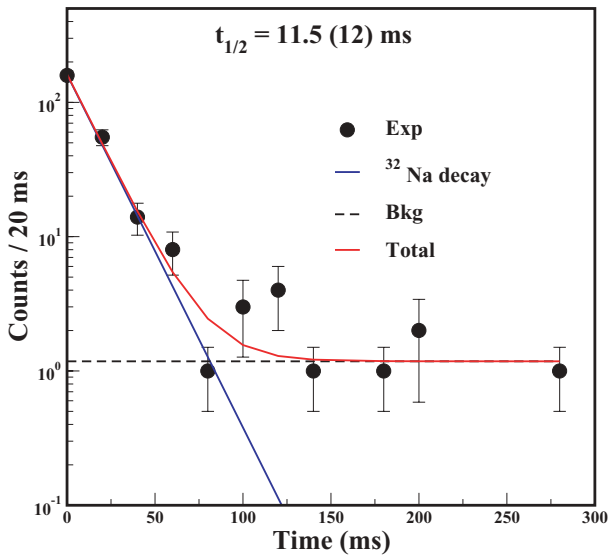

FIG. 5. (Color online) Decay time spectra for the 885 keV γ line in ^{32}Mg. The result of an exponential fit with a constant background gives a half-life of 11.5 (12) ms.

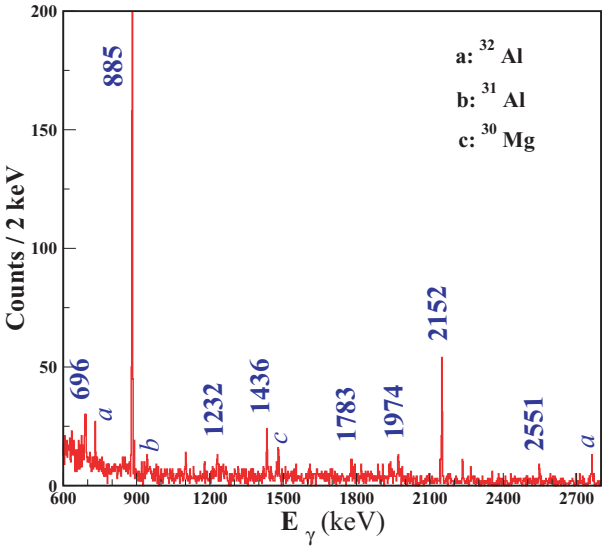

FIG. 6. (Color online) A partial β-delayed γ-ray spectrum for events coming within the first 60 ms after a ^{32}Na implantation, showing the important transitions in ^{32}Mg. The 485, 1666, 2269, and 3935 keV transitions with small intensities cannot be seen in this scale. γ rays from daughter and granddaughter activities are also indicated.

Q_β value, the γ decays observed would include decays in daughter and granddaughter nuclei produced in $0n$, $1n$, and $2n$ emissions. The short half-life of ^{32}Na ($\sim$13 ms), compared to the other nuclides in question, allowed us to isolate transitions in ^{32}Mg easily. A partial spectrum collected for 60 ms after the initial implantation is shown in Fig. 6, where the γ transitions in ^{32}Mg are indicated. Also seen are the strongest transitions in the grand daughter ^{32}Al (735 and 2765 keV [30]) from the β^- decay of ^{32}Mg. The intensities of the γ lines are listed in Table I.

III. DISCUSSION

The γ transitions in ^{32}Mg were identified from fragment-β-γ coincidences, as shown in Fig. 6. The decay curves of these transitions were found to be consistent with the measured half-life of ^{32}Mg, allowing for an unambiguous identification of these γ transitions. All the γ transitions seen in the present work have already been reported in the recent β-decay work of Mattoon *et. al.* [19], which was published at the time of analysis of this data. The excited levels in ^{32}Mg were created from the γ transitions keeping in mind that the intensity and energy sum rules were followed. Our analysis confirms the level scheme proposed in Ref. [19], which differs significantly from the earlier β-decay measurement of Klotz *et al.* [18]. The main difference lies in the placement of the 1232 keV transition, now feeding the 2321 keV level instead of the 885 keV state. With this reassignment of the 1232 keV transition, the 2117 keV level proposed in Ref. [18] is eliminated and the apparent β-decay strength into the 2321 keV state is decreased, which in turn increases the log ft value of this state. Also the 696 keV transition, though

TABLE I. Energies and intensities of γ transitions observed in the β decay of ^{32}Na. The absolute intensities were calculated using the total number of β-decaying implantations, 12065 (250), obtained from the fit shown in Fig 4.

E_γ (keV)	I_γ[a]	I_γ(%)	$E_i \rightarrow E_f$ (MeV)
51.0 (0.5)	17 (1)	10 (1)	0.051 $\rightarrow$ 0.0[b]
171.0 (0.5)	14 (1)	8 (1)	0.221 $\rightarrow$ 0.051[b]
221.0 (0.5)	9 (1)	5.5 (6)	[bc]
240.0 (0.5)	16 (1)	9 (1)	0.4611 $\rightarrow$ 0.221[b]
485.0 (1)	6 (1)	3.6 (6)	3.037 $\rightarrow$ 2.551
696.0 (1)	6 (1)	3.4 (6)	3.553 $\rightarrow$ 2.858
735.0 (0.5)	10 (2)	6 (1)	0.735 $\rightarrow$ 0.0[c]
885.0 (0.5)	100	58 (3)	0.885 $\rightarrow$ 0.0
895.0 (1)	3 (1)	1.6 (5)	0.945 $\rightarrow$ 0.051[b]
1232.0 (1)	10 (2)	6 (1)	3.553 $\rightarrow$ 2.321
1436.0 (1)	15 (2)	9 (1)	2.321 $\rightarrow$ 0.885
1482.0 (1)	12 (2)	7 (1)	1.482 $\rightarrow$ 0.0[d]
1666.0 (1)	2 (1)	0.9 (4)	2.551 $\rightarrow$ 0.885
1783.0 (1)	10 (2)	5.6 (11)	4.820 $\rightarrow$ 3.037
1974.0 (1)	13 (2)	7 (1)	2.858 $\rightarrow$ 0.885
2152.0 (1)	47 (4)	27 (3)	3.037 $\rightarrow$ 0.885
2269.0 (1)	4 (1)	2.2 (7)	4.820 $\rightarrow$ 2.551
2551.0 (1)	8 (2)	4.8 (11)	2.551 $\rightarrow$ 0.0
2765.0 (1)	38 (6)	22 (3)	2.765 $\rightarrow$ 0.0[c]
3935.0 (1.5)	18 (4)	10 (2)	4.820 $\rightarrow$ 0.885

[a]Intensities relative to the 885 keV γ transition in ^{32}Mg.
[b]Subsequent to β-delayed one-neutron emission, transition in ^{31}Mg.
[c]Decay of daughter nuclei, transition in ^{32}Al.
[d]Subsequent to β delayed two-neutron emission, transition in ^{30}Mg.

observed in Ref. [18], was not placed in the level scheme. It is now proposed to deexcite the level at 3.553 MeV created by the 1232 keV transition feeding the 2321 keV state, further strengthening the placement of the 1232 keV transition. The transitions at 485 and 2269 keV, not seen in Ref. [18], feed the 2551 keV level and lower its inferred β-decay strength compared with the earlier work. Additionally, the intensity of the 1974 keV γ line in the present work is about half of that quoted in Ref. [18], where it was obscured by a decay from ^{128}In, a contaminant. The level scheme from the present work is shown in Fig. 7, which agrees with that of Ref. [19] apart from the placement of the 4785 keV excited state.

The absolute intensities for β decay to the excited states in ^{32}Mg were calculated using the total number of β-decaying implants obtained from the fit to the total decay curve and the measured absolute efficiencies of the γ detectors. The direct feeding to the 2321 and 2551 kev states was found to be extremely small, in contrast to that of Ref. [18]. With the revised intensities, using the measured half-life for the β decay of ^{32}Na [13.1 (5) ms] and the Q_β values from Ref. [27], the apparent log ft values were calculated according to the prescription of Ref. [31]. For estimating the ground state branch, the β-delayed neutron emission probabilities P_{1n} and P_{2n} were taken from Ref. [18], 24 (7)% and 8 (2)%, respectively. The observed branches seem to exhaust almost all the β decay strength. However, keeping in mind that the neutron separation energy, S_n, in ^{32}Mg is 5.81 (2) MeV [27], there is a possibility that weak decays from high-lying states

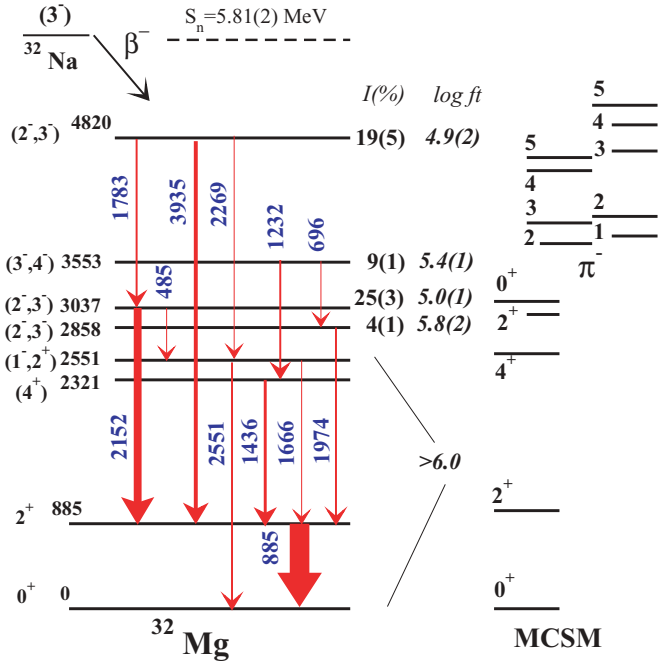

FIG. 7. (Color online) Apparent β-feeding intensities for the excited levels in ^{32}Mg observed in the present work. Intensity of the ground state was calculated using P_{1n} of 24(7)% and P_{2n} of 8(2)% from Ref. [18]. The apparent log ft values were calculated using the measured absolute intensities, half-life of 13.1 (5) ms, and Q_β value of 20019(357) keV [27] according to Ref. [31]. The proposed spin and parity assignments for the experimental levels are indicated on the left. Predictions of the MCSM calculations with the SDPF-M interaction are also shown. For MCSM, positive parity state levels above 0_2^+ are not shown for clarity. The negative parity states are labeled as π^-. All energies are in keV.

could not be observed. The apparent log ft values from the present work are key to understanding the nature of the excited states in the $N = 20$ nucleus ^{32}Mg.

The level structure was compared with the calculations in the sd shell model space with the USDA and USDB interactions [2]. As noted before, the energy of the 2^+ state is predicted way too high, in sharp contrast to the experimental result. To better reproduce the positive parity states for this $N = 20$ nucleus and to describe the negative parity states, which definitely involve excitation beyond the sd model space, MCSM calculations were performed. The valence space for the calculations is $d_{5/2}s_{1/2}d_{3/2}f_{7/2}p_{3/2}$ and the SDPF-M interaction [14,15] used in the calculations consists of three parts: USD and Kuo-Brown for the sd and fp shells and a cross shell interaction based on the Millener-Kurath interaction. The unique feature of the SDPF-M interaction is the significant variation of the $N = 20$ shell gap as a function of proton number from oxygen to silicon, achieved by modifying the monopole part of the interaction. There is no restriction about configurations in the given single-particle space and so all possible configurations are naturally mixed. Further details of the calculation can be found in Refs. [14] and [15] and the results are shown in Figs. 7 and 9 and Table II.

TABLE II. Experimental level energies compared with shell model calculations with the USDA interaction and the SDPF-M interaction. For the SDPF-M interaction the average number of fp shell neutrons is also given. All energies are in MeV.

J^π	$E_x^{\rm exp}$	$E_x^{\rm USDA}$[a]	$E_x^{\rm SDPF\text{-}M}$	$\langle\nu\rangle_{fp}$
0_1^+	0.0	0.0	0.0	2.2
2_1^+	0.885	1.6	0.98	2.2
4_1^+	2.321	2.6	2.63	2.1
2_2^+[b]	2.551	5.8	3.01	2.2
2_3^+	–	7.1	3.92	1.6
1_1^-	–	–	3.81	3.0
2_1^-[b]	2.858	–	3.76	3.0
3_1^-[b]	3.553	–	3.99	2.9
4_1^-	–	–	4.47	2.2
5_1^-	–	–	4.58	2.6
2_2^-[b]	3.037	–	3.94	3.0
3_2^-[b]	4.820	–	4.65	2.5
4_2^-	–	–	4.96	2.0
5_2^-	–	–	5.14	1.6
0_1^-	–	–	5.62	2.9

[a]Predictions for USDB similar.
[b]Tentative spin assignment.

A. Positive parity states

From simple shell model considerations, the ground state of the $N = 21$ parent nucleus ^{32}Na has negative parity. Hence allowed β transitions can only feed negative parity states (bound or unbound) in ^{32}Mg. The negligible branching to the known 0^+ ground state and the first 2^+ state at 885 keV in ^{32}Mg support the negative parity of ^{32}Na. The large apparent log ft values (>6) for the 2321 and 2551 keV states (Fig. 7), similar to the ground and the 885 keV states, suggest a forbidden nature of these β transitions also. Consistent with the positive parity of the ground state (0^+) and the state at 885 keV (2^+), positive parity is proposed for the 2321 and 2551 keV states, contrary to Ref. [18]. The 2321 keV state, which decays exclusively to the 2_1^+ state, is the most likely candidate for the 4_1^+ state as also suggested in Refs. [21] and [22]. The MCSM calculations [14] predict the 4_1^+ state at 2.63 MeV, in good agreement with the proposed state. This resolves the discrepancy around the 2321 keV state, which was long speculated to have positive parity though it could not be reconciled with the negative parity assignment of the earlier β-decay investigation [18]. With the 4^+ state proposed at 2.32 MeV, the ratio $\frac{E(4^+)}{E(2^+)}$ for ^{32}Mg can be extracted, and it turns out to be 2.6, similar to ^{26,28}Mg, and is in between the rigid rotor (3.3) and vibrational (2.0) estimates (see top panel of Fig. 8). This suggests that ^{32}Mg may not be an axially deformed rigid rotor as implied by the $B(E2 : 0^+ \rightarrow 2^+)$ measurement of Ref. [3]. The MCSM calculations also give a ratio of 2.7 between the 4^+ and the 2^+ states. Another way to explore the nature of the collectivity is to look at the $[E(4^+) - E(2^+)] - B(E2)$ correlations. The ratio $R4 = E(4^+)/E(2^+)$ is plotted against the measured

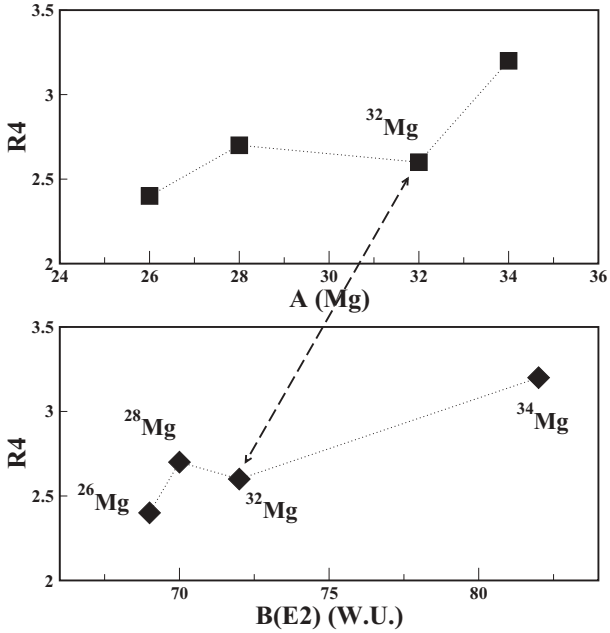

FIG. 8. (Top) Ratio of the energy of the 4_1^+ and 2_1^+ states ($R4$) for neutron-rich Mg isotopes, which is an indicator of the nature of collectivity of the isotope. (Bottom) Correlations between the measured ratio $R4$ with measured $B(E2)$ values for even-even Mg isotopes. ^{30}Mg is omitted as the 4^+ state is not known experimentally. The data are from http://www.nndc.bnl.gov/ensdf/.

$B(E2)$ values for the neutron-rich isotopes of Mg in Fig. 8 (bottom panel). A correlated increase of $R4$ and $B(E2)$ occurs for a deformed nucleus, as seems to be the case for ^{34}Mg. The trend seen in Fig. 8 thus suggests a more transitional nature for ^{32}Mg.

The state at 2.55 MeV is also proposed to have positive parity based on its log ft values and is the most likely candidate for the second 2^+ state predicted by the MCSM calculations at 3.01 MeV. However, this state has a dominant 2p-2h character (∼93%, Table II), though there were suggestions [21] of a spherical second 2^+ state earlier. The MCSM calculations predict the 2_3^+ state at ∼4.0 MeV to have less of a 2p-2h configuration. It should be noted here that a 1^- assignment for the 2551 keV state cannot be completely ruled out from the present experimental data as it would also imply a forbidden β transition.

B. Negative parity states

The states above 2.6 MeV have smaller log ft values, in the allowed range, and hence should have negative parity (Fig. 7), as the parent nucleus has negative parity. Before discussing the negative parity states, the spin assignment of ^{32}Na is revisited. Though the negative parity assignment for the ground state of ^{32}Na is supported by the absence of allowed decay to the first 0^+, 2^+, and proposed 4^+ states of ^{32}Mg, there is no experimental determination of the spin value. In the MCSM calculations the ground state can be 3^-, or 0^- similar to what was discussed in Ref. [18]. In the Nilsson model, the last proton has $\Omega = 3/2^+$, while the last neutron has $\Omega = 3/2^-$, which can couple to $K = 0^-$ or 3^-. In a deformed nucleus these will form two rotational bands. In the MCSM calculations the 0^- and 3^- states lie very close and hence there is a likelihood of a long-lived isomer arising from an $M3$ decay between them. In either case, the 3^- state would be strongly populated as the 2^- member of the $K = 0^-$ band prefers to decay to the 3^- via an $M1$ transition.

Back to the daughter nucleus, ^{32}Mg, as stated earlier, the states at 2.8, 3.0, 3.5, and 4.8 MeV are proposed to have negative parity. Based on the ground state spin-parity assumption of 3^- for ^{32}Na and the γ-decay pattern of these states to the positive parity states in ^{32}Mg (0^+, 2^+, and the proposed 4^+ states), the most likely possible spin values are indicated in Fig. 7. The results of the MCSM calculations are also shown in Fig. 7, which predict states in the spin range 2^- to 4^- that would be excellent candidates for the experimentally observed states. However, one does observe that the MCSM calculations predict the negative parity states to lie around 3.8 MeV; thus, an overestimate of about 1 MeV is seen for the calculations. Further, the distribution of the Gamow Teller strength [B(GT)] predicted by the MCSM calculation from a 3^- ground state of ^{32}Na is shown in Fig. 9. The β-decay feeding is predicted to go primarily to two 2^- states, the remaining strength being shared by the two 3^- states and the 4^- states having negligible β-decay strength. This β-decay pattern agrees qualitatively with the experimental observation of two strongly populated states. However, because the experimental spin assignments are tentative it is difficult to make a more explicit comparison. Still, one can say that the calculations overestimate the energies of the negative parity states. The present data thus provide important constraints to refine the calculations.

Among the nearby $N = 20$ isotones, negative parity states have been established in ^{34}Si [32], lying above 4.2 MeV. The drop in excitation energy for the negative parity states in ^{32}Mg can be explained if the $d_{3/2} - f_{7/2}$ shell gap varies with Z,

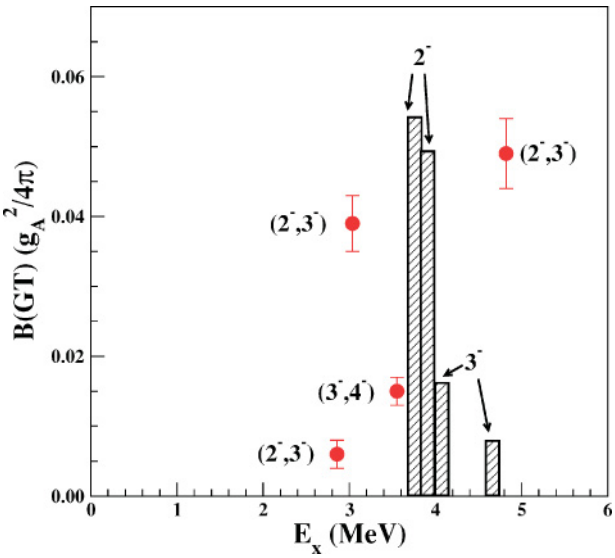

FIG. 9. (Color online) The experimental and calculated B(GT) strength in the β^- decay of ^{32}Na. The B(GT) was estimated in the MCSM calculations (histogram) by assuming a $J^\pi = 3^-$ for the ground state of ^{32}Na with a 2p-2h configuration and is scaled down by the quenching factor 0.7 [33].

becoming smaller for lower Z, as is assumed in the MCSM calculations. As an extrapolation, the negative parity states would drop further in ^{30}Ne. However, this awaits experimental verification.

Regarding the nature of the negative parity states observed in ^{32}Mg, a nucleus inside the island of inversion, both normal (1p-1h) and intruder (3p-3h) negative parity states are expected as a consequence of the smaller $N = 20$ shell gap. It is predicted [16], however, that a smaller shell gap would tend to favor the yrast negative parity states to be dominated by 3p-3h configurations (see Table II). This competition between 1p-1h and 3p-3h can be compared to the competition between 0p-0h and 2p-2h positive parity states. However, this prediction has not yet been tested, as negative parity states have not been identified unambiguously in the $N = 20$ isotones for $Z \sim 11$. In the present case, ^{32}Na with $N = 21$ is a nucleus inside the island of inversion with a dominant 2p-2h configuration in its ground state, manifested in its anomalous binding energy [8]. This implies an average population of three neutrons in the fp shell, as also predicted by the MCSM calculations (two being excited from across the $N = 20$ shell gap). The β^- decay (Gamow Teller transformation) from such a state would entail the conversion of a $\nu d_{3/2}$ neutron to a $\pi d_{5/2}$ proton, favored by energy and transition matrix elements. Such a transition would create 3p-3h states with negative parity in the daughter nucleus, ^{32}Mg. Thus, the negative parity states in ^{32}Mg identified in the present work (Fig. 7) must have an intruder 3p-3h character. This supports the predictions of the MCSM calculation where the yrast negative states are of 3p-3h character and lie above 3.8 MeV (see Table II). The normal 1p-1h negative parity states are expected to lie even higher. This *inversion* for the negative parity states, similar to the inversion between 0p-0h and 2p-2h states, highlights the quenching of the $N = 20$ gap.

IV. SUMMARY

The β-decay study of ^{32}Na presented in this article helped to revise the spin and parity assignments of the excited states in ^{32}Mg. The level at 2.321 MeV is now assigned a 4^+ spin and parity, resulting in $E(4^+)/E(2^+) \sim 2.6$, resolving a long-standing discrepancy about the parity of this state. Comparison of the experimental level structure was made with Monte Carlo shell model calculations using the SDPF-M interaction in the sd-$p_{3/2}f_{7/2}$ valence space. The comparison helped us to identify the 3p-3h intruder negative parity states, which lie below the 1p-1h states, displaying an inversion for the negative parity states similar to that seen in the positive parity states between 0p-0h and 2p-2h in the island of inversion. This inversion is a clear indicator of the reduced $N = 20$ shell gap for the nuclei around ^{32}Mg. The calculations, however, overestimate the negative parity states, which together with the discrepancy in reproducing the 2p-2h ground state of ^{31}Mg points to the further needed refinement of the interaction.

ACKNOWLEDGMENTS

The authors appreciate the NSCL operations staff for their help. This work was supported by NSF Grants PHY-04-56463 and PHY-06-06007 and in part by a Grant-in-Aid for Specially Promoted Research (13002001) from the MEXT of Japan.

[1] C. Detraz, D. Guillemaud, G. Huber, R. Klapisch, M. Langevin, F. Naulin, C. Thibault, L. C. Carraz, and F. Touchard, Phys. Rev. C **19**, 164 (1979).
[2] B. A. Brown and B. H. Wildenthal, Annu. Rev. Nucl. Part. Sci. **38**, 29 (1998); B. A. Brown and W. A. Richter, Phys. Rev. C **74**, 034315 (2006).
[3] T. Motobayashi, Y. Ikeda, Y. Ando, K. Ieki, M. Inoue, N. Iwasa, T. Kikuchi, M. Kurokawa, S. Moriya, S. Ogawa, H. Murakami, S. Shimoura, Y. Yanagisawa, T. Nakamura, Y. Watanabe, M. Ishihara, T. Teranishi, H. Okuno, and R. F. Casten, Phys. Lett. **B346**, 9 (1995).
[4] B. V. Pritychenko, T. Glasmacher, P. D. Cottle, M. Fauerbach, R. W. Ibbotson, K. W. Kemper, V. Maddalena, A. Navin, R. Ronningen, A. Sakharuk, H. Scheit, and V. G. Zelevinsky, Phys. Lett. **B461**, 322 (1999).
[5] H. Iwasaki, T. Motobayashi, H. Sakurai, K. Yoneda, T. Gomi, N. Aoi, N. Fukuda, Zs. Fulop, U. Futakami, Z. Gacsi, Y. Higurashi, N. Imai, N. Iwasa, T. Kubo, M. Kunibu, M. Kurokawa, Z. Liu, T. Minemura, A. Saito, M. Serata, S. Shimoura, S. Takeuchi, Y. X. Watanabe, K. Yamada, Y. Yanagisawa, and M. Ishihara, Phys. Lett. **B522**, 227 (2001).
[6] G. Neyens, M. Kowalska, D. Yordanov, K. Blaum, P. Himpe, P. Lievens, S. Mallion, R. Neugart, N. Vermeulen, Y. Utsuno, and T. Otsuka, Phys. Rev. Lett. **94**, 022501 (2005).
[7] Y. Yanagisawa, M. Notani, H. Sakurai, M. Kunibu, H. Akiyoshi, N. Aoi, H. Baba, K. Demichi, N. Fukuda, H. Hasegawa, Y. Higurashi, M. Ishihara, N. Iwasa, H. Iwasaki, T. Gomi, S. Kanno, M. Kurokawa, Y. U. Matsuyama, S. Michimasa, T. Minemura, T. Mizoi, T. Nakamura, A. Saito, M. Serata, S. Shimoura, T. Sugimoto, E. Takeshita, S. Takeuchi, K. Ue, K. Yamada, K. Yoneda, and T. Motobayashi, Phys. Lett. **B566**, 84 (2003).
[8] C. Thibault, R. Klapisch, C. Rigaud, A. M. Poskanzer, R. Prieels, L. Lessard, and W. Reisdorf, Phys. Rev. C **12**, 644 (1975).
[9] G. Huber, F. Touchard, S. Buttgenbach, C. Thibault, R. Klapisch, H. T. Duong, S. Liberman, J. Pinard, J. L. Vialle, P. Juncar, and P. Jacquinot, Phys. Rev. C **18**, 2342 (1978).
[10] E. K. Warburton, J. A. Becker, and B. A. Brown, Phys. Rev. C **41**, 1147 (1990).
[11] H. Sakurai, S. M. Lukyanov, M. Notani, N. Aoi, D. Beaumel, N. Fukuda, M. Hirai, E. Ideguchi, N. Imai, M. Ishihara, H. Iwasaki, T. Kubo, K. Kusaka, H. Kumagai, T. Nakamura, H. Ogawa, Yu. E. Penionzhkevich, T. Teranishi, Y. X. Watanabe, K. Yoneda, and A. Yoshida, Phys. Lett. **B448**, 180 (1999).
[12] P. D. Stevenson, J. Rikovska Stone, and M. R. Strayer, Phys. Lett. **B545**, 291 (2002).
[13] E. Caurier, F. Nowacki, and A. Poves, Nucl. Phys. **A693**, 374 (2001).
[14] Y. Utsuno, T. Otsuka, T. Mizusaki, and M. Honma, Phys. Rev. C **60**, 054315 (1999).
[15] Y. Utsuno, T. Otsuka, T. Glasmacher, T. Mizusaki, and M. Honma, Phys. Rev. C **70**, 044307 (2004).

[16] T. Otsuka, R. Fujimoto, Y. Utsuno, B. A. Brown, M. Honma, and T. Mizusaki, Phys. Rev. Lett. **87**, 082502 (2001).
[17] T. Otsuka, T. Suzuki, R. Fujimoto, H. Grawe, and Y. Akaishi, Phys. Rev. Lett. **95**, 232502 (2005).
[18] G. Klotz, P. Baumann, M. Bounajma, A. Huck, A. Knipper, G. Walter, G. Marguier, C. Richard-Serre, A. Poves, and J. Retamosa, Phys. Rev. C **47**, 2502 (1993).
[19] C. M. Mattoon, F. Sarazin, G. Hackman, E. S. Cunningham, R. A. E. Austin, G. C. Ball, R. S. Chakrawarthy, P. Finlay, P. E. Garrett, G. F. Grinyer, B. Hyland, K. A. Koopmans, J. R. Leslie, A. A. Phillips, M. A. Schumaker, H. C. Scraggs, J. Schwarzenberg, M. B. Smith, C. E. Svensson, J. C. Waddington, P. M. Walker, B. Washbrook, and E. Zganjar, Phys. Rev. C **75**, 017302 (2007).
[20] S. Nummela, F. Nowacki, P. Baumann, E. Caurier, J. Cederkall, S. Courtin, P. Dessagne, A. Jokinen, A. Knipper, G. Le Scornet, L. G. Lyapin, Ch. Miehe, M. Oinonen, E. Poirer, Z. Radivojevic, M. Ramdhane, W. H. Trzaska, G. Walter, and J. Aysto (ISOLDE Collaboration), Phys. Rev. C **64**, 054313 (2001).
[21] F. Azaiez, M. Belleguic, D. Sohler, M. Stanoiu, Zs. Dombradi, O. Sorlin, J. Timar, F. Amorini, D. Baiborodin, A. Bauchet, F. Becker, C. Borcea, C. Bourgeois, Z. Dlouhy, C. Donzaud, J. Duprat, D. Guillemaud-Mueller, F. Ibrahim, M. J. Lopez, R. Lucas, S. M. Lukyanov, V. Maslov, J. Mrazek, C. Moore, F. Nowacki, B. M. Nyako, Yu.-E. Penionzhkevich, M. G. Saint-Laurent, F. Sarazin, J. A. Scarpaci, G. Sletten, C. Stodel, M. Taylor, C. Theisen, and G. Voltolini, Eur. Phys. J. A **15**, 93 (2002).
[22] D. Bazin, B. A. Brown, C. M. Campbell, J. A. Church, D. C. Dinca, J. Enders, A. Gade, T. Glasmacher, P. G. Hansen, W. F. Mueller, H. Olliver, B. C. Perry, B. M. Sherrill, J. R. Terry, and J. A. Tostevin Phys. Rev. Lett. **91**, 012501 (2003).
[23] W. Mittig, H. Savajols, D. Baiborodin, J. M. Casandjian, C. E. Demonchy, P. Roussel-Chomaz, F. Sarazin, Z. Dlouhy, J. Mrazek, A. V. Belozyorov, S. M. Lukyanov, Y. E. Penionzhkevich, N. Alamanos, A. Drouart, A. Gillibert, C. Jouanne, V. Lapoux, E. Pollacco, A. Korichi, and J. A. Scarpaci, Eur. Phys. J. A **15**, 157 (2002).
[24] S. Takeuchi, N. Aoi, H. Baba, T. Fukui, Y. Hashimoto, K. Ieki, N. Imai, H. Iwasaki, S. Kanno, Y. Kondo, T. Kubo, K. Kurita, T. Minemura, T. Motobayashi, T. Nakabayashi, T. Nakamura, T. Okumura, T. K. Onishi, S. Ota, H. Sakurai, S. Shimoura, R. Sugou, D. Suzuki, H. Suzuki, M. K. Suzuki, E. Takeshita, M. Tamaki, K. Tanaka, Y. Togano, and K. Yamada, J. Phys.: Conf. Ser. **49**, 153 (2006).
[25] D. J. Morrissey, B. M. Sherrill, M. Steiner, A. Stolz, and I. Wiedenhover, Nucl. Instrum. Methods Phys. Res. B **204**, 90 (2003).
[26] J. I. Prisciandaro, A. C. Morton, and P. F. Mantica, Nucl. Instrum. Methods Phys. Res. A **505**, 140 (2003).
[27] G. Audi, A. H. Wapstra, and C. Thibault, Nucl. Phys. **A729**, 337 (2003).
[28] M. Langevin, C. Dtraz, D. Guillemaud-Mueller, A. C. Mueller, C. Thibault, and F. Touchard, Nucl. Phys. **A414**, 151 (1984).
[29] W. F. Mueller, J. A. Church, T. Glasmacher, D. Gutknecht, G. Hackman, P. G. Hansen, Z. Hu, K. L. Miller, and P. Quirin, Nucl. Instrum. Methods Phys. Res. A **466**, 492 (2003).
[30] S. Grevy, S. Pietri, L. Achouri, J. C. Angelique, P. Baumann, C. Borcea, A. Buta, W. Catford, S. Courtin, J. M. Daugas, F. De Oliveira, P. Dessagne, Z. Dlouhy, D. Guillemaud-Mueller, R. Hadeler, A. Knipper, F. R. Lecolley, J. L. Lecouey, M. Lewitowicz, E. Lienard, C. Miehe, J. Mrazek, F. Negoita, N. A. Orr, Y. Penionzhkevich, J. Peter, E. Poirier, M. Stanoiu, O. Tarasov, C. Timis, and G. Walter, Nucl. Phys. **A734**, 369 (2004).
[31] N. B. Gove and M. J. Martin, Nucl. Data Tables A **10**, 205 (1971).
[32] S. Nummela, P. Baumann, E. Caurier, P. Dessagne, A. Jokinen, A. Knipper, G. Le Scornet, C. Miehe, F. Nowacki, M. Oinonen, Z. Radivojevic, M. Ramdhane, G. Walter, and J. Aysto (ISOLDE Collaboration), Phys. Rev. C **63**, 044316 (2001).
[33] B. H. Wildenthal, M. S. Curtin, and B. A. Brown, Phys. Rev. C **28**, 1343 (1983).